

DOI:10.1002/ejic.201403125

Li₁₄(PON₃)₂O – A Non-Condensed Oxonitridophosphate Oxide

Dominik Baumann^[a] and Wolfgang Schnick*^[a]

Keywords: Lithium / Phosphorus / Nitrides / Solid-state reactions / Solid-state structures

Li₁₄(PON₃)₂O was synthesized by reaction of phosphoric triamide PO(NH₂)₃ with LiNH₂ at 550 °C. It crystallizes in a trigonal structure [*P* $\bar{3}$ (no. 147), *a* = 5.6880(5), *c* = 8.0855(8) Å, *V* = 226.55(5) Å³, *Z* = 1] that can be described as a defect variant of the antiferroite structure type. The crystal structure was elucidated from X-ray powder diffraction data and cor-

roborated by FTIR and solid-state NMR spectroscopy. Li₁₄(PON₃)₂O is composed of non-condensed PON₃⁶⁻ tetrahedra and O²⁻ ions that are surrounded by tetrahedrally coordinated Li⁺. This is the first example of an *ortho*-oxonitridophosphate.

Introduction

Over the past few decades, nitridophosphates and oxonitridophosphates have received renewed interest due to their large structural variability. The parent compounds P₃N₅,^[1] PON,^[2] and PN(NH)^[3] have been known since the 18th century. However, owing to intrinsic difficulties in crystal growth, comprehensive structural descriptions were not possible until the advent of modern powder diffraction techniques.^[4–6]

Due to the fact that both PON and PN(NH) are isoelectronic to SiO₂,^[7] (oxo)nitridophosphates and silicates often display similar structural features. Many of the well-studied structures of SiO₂ have also been found in PON, such as the cristobalite,^[8] quartz,^[9] and coesite structure types.^[10] Structures comparable to layer and chain silicates are found in Sr₂P₆O₆N₈^[11] and M₂PN₃ (M = Ca, Mg, Zn).^[12,13] The high structural flexibility of (oxo)nitridophosphates may partly be caused by the fact that more than two tetrahedra can be linked by the nitride ion. This is expressed by remarkable building blocks such as the star-shaped N(PO₃)₃⁶⁻ ion^[14] or the adamantane analogue P₄N₁₀¹⁰⁻ ion in Li₁₀P₄N₁₀.^[15] However, with Li₇PN₄, there is only one example of a nitridophosphate-containing isolated tetrahedra.^[16] This is in stark contrast to the varied and extensive range of known *ortho*-silicates. Presumably, Li⁺ is especially suitable for stabilization of highly charged *ortho*-anions such as PN₄⁷⁻.

Lithium oxonitridophosphates, in particular, have attracted attention as possible lithium ion conductors. Such

compounds already enjoy application in the form of amorphous LiPON thin films.^[17] A variety of possible structural candidates for Li₂PO₂N have been predicted by Holzwarth et al.^[18] on the basis of ab initio calculations, which closely resemble those verified by experiment.^[19]

In this contribution, we report on the successful preparation of Li₁₄(PON₃)₂O, the first *ortho*-oxonitridophosphate, containing isolated PON₃⁶⁻ tetrahedra beside O²⁻ ions, synthesized by using a molecular precursor.

Results and Discussion

Nearly phase-pure samples of Li₁₄(PON₃)₂O were obtained by high-temperature reaction of phosphoric triamide PO(NH₂)₃ and LiNH₂ in evacuated silica glass ampoules. The samples were microcrystalline, colorless, and sensitive to moisture.

The crystal structure of Li₁₄(PON₃)₂O (Figure 1) was elucidated by ab initio calculations with the charge-flipping algorithm using X-ray powder diffraction data (Figure 1). The presence of elements other than Li, P, O and N was ruled out on the basis of energy dispersive X-ray (EDX) spectroscopy. Rietveld refinement showed only small amounts of an unidentified side phase. Assignment of the anion positions to O and N in an ordered way was carried out on the basis of their isotropic displacement parameters. Different distributions lead to significantly abnormal values, thus giving a strong indication that the structural model is correct. Additionally, this distribution of O and N leads to an electrically neutral structure as well as to the occurrence of the expected PON₃⁶⁻ ion. The positions of Li⁺ were determined from difference Fourier maps.

Li₁₄(PON₃)₂O crystallizes in the trigonal space group *P* $\bar{3}$ with the lattice parameters *a* = 5.6880(5) Å and *c* = 8.0855(8) Å. Further crystallographic data are summarized

[a] Department Chemie, Lehrstuhl für Anorganische Festkörperchemie, Ludwig-Maximilians-Universität München Butenandtstrasse 5–13, 81377 München, Germany
E-mail: wolfgang.schnick@uni-muenchen.de
<http://www.cup.uni-muenchen.de/ac/schnick>

Supporting information for this article is available on the WWW under <http://dx.doi.org/10.1002/ejic.201403125>.

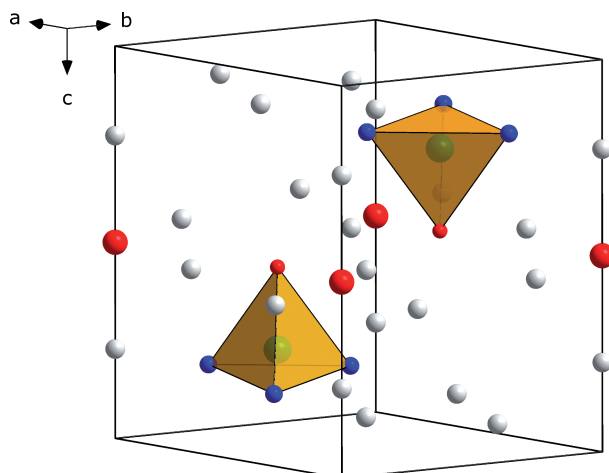


Figure 1. Crystal structure of $\text{Li}_{14}(\text{PON}_3)_2\text{O}$ (P: green, O: red, N: blue, Li: white).

in Table 1 and atomic positions and isotropic displacement parameters are given in Table 2. The crystal structure (Figure 2) is isotypic to $\text{Li}_{14}\text{Cr}_2\text{N}_8\text{O}^{[20,21]}$ and $\text{Na}_{14}\text{Mn}_2\text{O}_9$,^[22] albeit with a different anion arrangement. The crystal structure can be understood as a defect variant of the anti-fluorite structure type. O^{2-} and N^{3-} ions are arranged in a slightly distorted cubic closest packing, whereas 16/18 of the tetrahedral voids are occupied by P^{5+} and Li^+ , respectively. For every tetrahedral void occupied by P, one of the adjacent tetrahedral voids along [001] is unoccupied. Due to the occurrence of isolated PON_3^{6-} tetrahedra as well as isolated O^{2-} ions, $\text{Li}_{14}(\text{PON}_3)_2\text{O}$ can be considered a lithium oxonitridophosphate oxide. As detailed by Rabenau et al., the cubic cell of the anti-fluorite structure of Li_2O can be transformed to the trigonal cell found in $\text{Li}_{14}(\text{PON}_3)_2\text{O}$.^[20]

Transforming the unit cell of Li_2O in this manner results in a trigonal cell with lattice parameters $a = 5.6510 \text{ \AA}$ and $c = 7.9917 \text{ \AA}$. These values, and consequently the cell vol-

Table 1. Crystal data for $\text{Li}_{14}(\text{PON}_3)_2\text{O}$.

Formula	$\text{Li}_{14}(\text{PON}_3)_2\text{O}$
Formula mass [g mol^{-1}]	291.16
Crystal system / space group	trigonal, $P\bar{3}$ (no. 147)
Lattice parameters [\AA]	$a = 5.6880(5)$ $c = 8.0855(8)$
Cell volume [\AA^3]	226.55(5)
Formula units per cell Z	1
X-ray density [g cm^{-3}]	2.147
Linear absorption coefficient [cm^{-1}]	43.39
Radiation	$\text{Cu-K}\alpha_1$ ($\lambda = 154.059 \text{ pm}$)
Monochromator	Ge(111)
Diffractometer	Stoe StadiP
Detector	MYTHEN 1K
2θ range [$^\circ$]	5–110.51
Temperature [K]	297(2)
Data points	7035
Number of observed reflections	198
Number of parameters	52
Constraints	0
Program used	TOPAS Academic
Structure solution	charge-flipping
Structure refinement	Rietveld method
Profile function	fundamental parameters model
Background function	shifted Chebyshev
R_{wp}	0.07553
R_{exp}	0.01776
R_{p}	0.04576
R_{Bragg}	0.01539
χ^2	4.252

Table 2. Atomic coordinates and isotropic equivalent displacement parameters for $\text{Li}_{14}(\text{PON}_3)_2\text{O}$.

Atom	Wyckoff symbol	x	y	z	U_{iso} [\AA^2]
P1	$2d$	1/3	2/3	0.2379(6)	0.0074(6)
O1	$1b$	1/3	2/3	0.4482(9)	0.029(2)
O2	$2d$	0	0	1/2	0.044(4)
N1	$6g$	0.057(2)	0.6919(8)	0.1736(8)	0.023(2)
Li1	$6g$	0.045(3)	0.636(3)	0.909(2)	0.034(5)
Li2	$6g$	0.293(3)	0.291(3)	0.411(2)	0.037(4)
Li3	$2c$	0	0	0.77(1)	0.17(2)

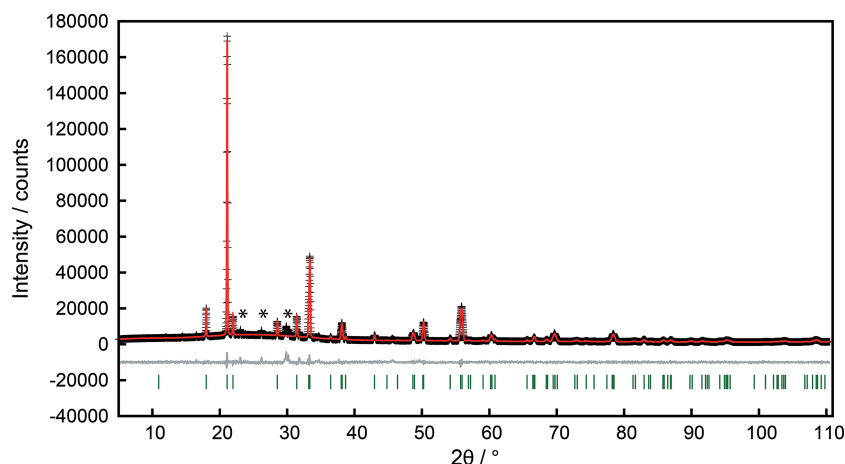


Figure 2. Observed (crosses) and calculated (red line) powder diffraction pattern of $\text{Li}_{14}(\text{PON}_3)_2\text{O}$ as well as position of Bragg reflections (green ticks) and difference profile (gray line). Reflections from an unknown side phase are marked with asterisks.

ume of 221.01 Å³, are very close to the values found for Li₁₄(PON₃)₂O (*a* = 5.6880 Å and *c* = 8.0855 Å, *V* = 226.55 Å³). The slightly larger cell dimensions of the title compound are presumably due to the slightly larger ionic radius of N³⁻ (146 pm) compared with O²⁻ (138 pm).^[23] The “isolated” oxygen atom O2 is coordinated by eight Li atoms in the form of a slightly distorted cube, whereas, due to the incomplete filling of the tetrahedral voids, O1 and N1 are coordinated in the shape of a cube with one of its vertices removed. This coordination polyhedron resembles a highly distorted capped trigonal bipyramid.

Atomic arrangements and bond lengths in Li₁₄(PON₃)₂O are displayed in Figure 3. Bond lengths around P are 170.0(9) pm to O and 172.8(7) pm to N. These values are comparable to the value of 173.3 pm found in closely related Li₇PN₄,^[16] but significantly longer than those found in PO(NH₂)₃,^[24] which can be explained by the higher charge of the PON₃⁶⁻ ion. With values between 107.5(3) and 111.4(3)°, O/N–P–O/N angles differ only slightly from the regular tetrahedral angle. Bond lengths around Li differ greatly due to the different properties of the coordinating anions. Distances between Li and the isolated O2 (181–220 pm) and N1 (178–227 pm) are shorter than those to O1 (205–231 pm). The variation of these distances may be due to the more covalent nature of the P–N bonds and its small variability in length, which leads to a distortion of the Li(O,N)₄ tetrahedra.

To prove complete deprotonation of PO(NH₂)₃ to PON₃⁶⁻, and the consequential absence of H as described by the structural model, FTIR spectroscopy was performed. The spectrum (Figure 4) shows only a very weak signal in the region where N–H vibrations are expected, which can be explained by surface hydrolysis of the sample. However, the presence of stoichiometric amounts of hydrogen in the sample seems to be unlikely. P–O and P–N vibrations are visible in the region between 500 and 1000 cm⁻¹.

Solid-state NMR spectroscopy was used to corroborate the crystal structure model. The ³¹P NMR spectrum shows a single strong resonance at δ = 44.3 ppm. Small peaks between 25 and 0 ppm are caused by trace amounts of a side

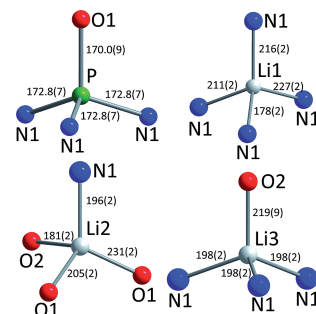


Figure 3. Interatomic distances (pm) in Li₁₄(PON₃)₂O.

phase present in the sample. The single comparatively broad resonance can be attributed to the single crystallographic P site in the structural model. The large line width might be caused by cross-terms between the quadrupole interaction of the ¹⁴N (*I* = 1) and the dipolar coupling between ¹⁴N and ³¹P, which are in close proximity. The measured chemical shift is close to that observed for Li₇PN₄ (δ = 49.2, 54.6 ppm).^[25] This suggests that the range of chemical shifts of *ortho*-(oxo)nitridophosphates is around 40–

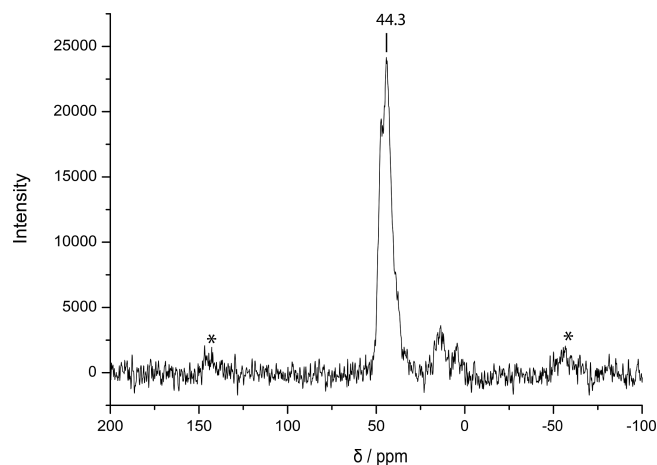


Figure 5. ³¹P solid-state NMR spectrum of Li₁₄(PON₃)₂O at 20 kHz MAS. Rotational sidebands are marked with asterisks.

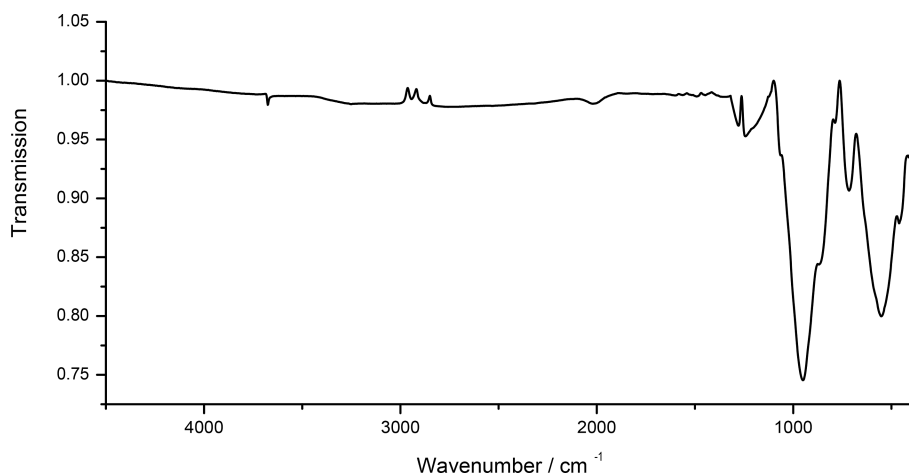


Figure 4. FTIR spectrum of Li₁₄(PON₃)₂O.

60 ppm. The ^7Li solid-state NMR spectrum (Figure S1 in the Supporting Information) shows a single broad resonance at a chemical shift of 2.3 ppm that is a superposition of the crystallographically verified three distinct Li sites (Figure 5).

Conclusions

The crystal structure of $\text{Li}_{14}(\text{PON}_3)_2\text{O}$ was elucidated by using powder diffraction data. This is the first example of an *ortho*-oxonitridophosphate. Due to the chemical similarity to the *ortho*-nitridophosphate Li_7PN_4 , both compounds share structural similarities and both can be formally derived from the antifluorite structure type of Li_2O . The PON_3^{6-} ion in this compound can be thought of as the full deprotonation product of phosphoric triamide $\text{PO}(\text{NH}_2)_3$. By varying the stoichiometric ratio of LiNH_2 and $\text{PO}(\text{NH}_2)_3$, a wide range of further lithium oxonitridophosphates with varying degrees of condensation might theoretically be accessible. The synthesis route of high-temperature deprotonation might thus be applicable for future synthesis of further new oxonitridophosphate materials. Given that related compounds $\text{Li}_3\text{N}^{[26]}$ and $\text{Li}_7\text{PN}_4^{[27]}$ show significant lithium-ion conductivity, further investigations concerning the ionic conductivity of $\text{Li}_{14}(\text{PON}_3)_2\text{O}$ might be advisable in the future.

Experimental Section

General: All manipulations were performed under exclusion of oxygen and moisture using either standard air-free techniques in flame-dried glassware attached to a vacuum line, or in an Ar-filled glove box (< 1 ppm O_2 , < 0.1 ppm H_2O , MBRAUN, Garching, Germany). Silica glass ampoules were sealed under dynamic vacuum using an oxyhydrogen torch.

Phosphoric triamide $\text{PO}(\text{NH}_2)_3$ was synthesized from POCl_3 and liquid NH_3 according to the procedure described by Klement and Koch.^[28] POCl_3 (15 mL) was slowly added to liquid NH_3 (150 mL) at -78 °C. The resulting suspension was stirred for 1 h and the excess NH_3 was evaporated. To separate the mixture of $\text{PO}(\text{NH}_2)_3$ and NH_4Cl , the mixture was heated to reflux with an excess of Et_2NH in CH_2Cl_2 until the evolution of NH_3 ceased. Pure $\text{PO}(\text{NH}_2)_3$ was then obtained by filtration from the suspension. The purity of the product was confirmed by powder X-ray diffraction.

Synthesis of $\text{Li}_{14}(\text{PON}_3)_2\text{O}$: $\text{PO}(\text{NH}_2)_3$ (23.8 mg, 0.25 mmol) and LiNH_2 (34.4 mg, 1.5 mmol, 95%, Sigma–Aldrich) were thoroughly mixed in an agate mortar and filled into an evacuated silica glass ampoule, which was then placed in the center of a tube furnace. The temperature was raised to 550 °C at a rate of 15 K/h, held for 24 h and subsequently lowered to room temperature at 60 K/h. The product was obtained as a colorless, moisture-sensitive powder.

Powder X-ray Diffraction: Powder diffraction was carried out in parafocusing Debye–Scherrer geometry with a StadiP diffractometer (Stoe, Darmstadt, Germany) using $\text{Ge}(111)$ -monochromated $\text{Cu-K}_{\alpha 1}$ radiation and a MYTHEN 1K. The sample was enclosed in glass capillary ($\varnothing 0.5$ mm). Structure solution and refinement on powder data were carried out using TOPAS Academic 4.1.^[29] Indexing of the powder pattern was achieved by using the

SVD-Algorithm.^[30] After intensity extraction using the Pawley method, the structure was solved ab initio using the charge flipping algorithm.^[31] During subsequent Rietveld refinement, the peak shapes were modeled by using the fundamental parameters approach (direct convolution of source emission profiles, axial instrument contributions and crystallite size and microstrain effects).^[32] The background was modeled as a Chebychev polynomial. Absorption effects were corrected by modeling a cylindrical sample with a packing density of 0.7. Preferred orientation was corrected by spherical harmonics functions of the 4th order.^[33] Further details of the crystal structure investigation can be obtained from the Fachinformations-Zentrum Karlsruhe, 76344 Eggenstein-Leopoldshafen, Germany [Fax: (+49)7247-808-259; E-mail: crysdata@fiz-karlsruhe.de] on quoting the depository number CSD-428737.

Spectroscopic Methods: FTIR spectroscopy was carried out with an IFS 66 v/S spectrometer (Bruker) using KBr disks. Solid-state NMR spectra were collected with a Bruker Avance III spectrometer equipped with an 11.7 T magnet and a 2.5 mm MAS probe at a spinning rate of 20 kHz, using direct excitation. Chemical shift values are referenced to 0.1% TMS in CDCl_3 (Sigma–Aldrich) as an external reference. Energy dispersive X-ray (EDX) spectroscopy was carried out with a Jeol JSM-6500F scanning electron microscope equipped with an Oxford Instruments Si/Li 7418 EDX detector.

Supporting Information (see footnote on the first page of this article): Full details of interatomic distances, ^7Li solid-state NMR spectrum, and a larger version of the Rietveld plot.

Acknowledgments

The authors gratefully acknowledge financial support from the Fonds der Chemischen Industrie (FCI). The authors thank Christian Minke and Dr. Thomas Bräuniger, both Department of Chemistry LMU Munich, for help with the NMR and EDX measurements.

- [1] H. Rose, *Ann. Pharm.* **1834**, *11*, 129–139; H. Rose, *Ann. Pharm.* **1834**, *11*, 139–150.
- [2] J. H. Gladstone, *Q. J. Chem. Soc.* **1862**, *14*, 121–131.
- [3] M. C. Gerhardt, *Ann. Chim. Phys.* **1846**, *18*, 188.
- [4] a) S. Horstmann, E. Irran, W. Schnick, *Angew. Chem. Int. Ed. Engl.* **1997**, *36*, 1873–1875–1940; *Angew. Chem.* **1997**, *109*, 1938; b) S. Horstmann, E. Irran, W. Schnick, *Z. Anorg. Allg. Chem.* **1998**, *624*, 620–628.
- [5] K. R. Waerstad, J. M. Sullivan, *J. Appl. Crystallogr.* **1976**, *9*, 411.
- [6] W. Schnick, J. Lücke, *Z. Anorg. Allg. Chem.* **1992**, *610*, 121–126.
- [7] A. Le Sauze, J. Haines, C. Chateac, J. M. Leger, R. Marchand, *Mater. Sci. Forum* **2000**, 325–326, 77–82.
- [8] J. M. Léger, J. Haines, C. Chateau, G. Bocquillon, M. W. Schmidt, S. Hull, F. Gorelli, A. Lesauze, R. Marchand, *Phys. Chem. Miner.* **2001**, *28*, 388–398.
- [9] J. M. Léger, J. Haines, L. S. de Oliveira, C. Chateau, A. Le Sauze, R. Marchand, S. Hull, *J. Phys. Chem. Solids* **1999**, *60*, 145–152.
- [10] D. Baumann, W. Schnick, unpublished results.
- [11] S. J. Sedlmaier, J. Schmedt auf der Günne, W. Schnick, *Dalton Trans.* **2009**, 4081–4084.
- [12] V. Schultz-Coulon, W. Schnick, *Z. Anorg. Allg. Chem.* **1997**, *623*, 69–74.
- [13] S. J. Sedlmaier, M. Eberspächer, W. Schnick, *Z. Anorg. Allg. Chem.* **2011**, *637*, 362–367.
- [14] R. Conanec, W. Feldmann, R. Marchand, Y. Laurent, *J. Solid State Chem.* **1996**, *121*, 418–422.

- [15] W. Schnick, U. Berger, *Angew. Chem. Int. Ed. Engl.* **1991**, *30*, 830–831; *Angew. Chem.* **1991**, *103*, 857–858.
- [16] W. Schnick, J. Lücke, *J. Solid State Chem.* **1990**, *87*, 101–106.
- [17] J. B. Bates, N. J. Dudney, G. R. Gruzalski, R. A. Zuhr, A. Choudhury, C. F. Luck, J. D. Robertson, *J. Power Sources* **1993**, *43*, 103–110.
- [18] Y. A. Du, N. A. W. Holzwarth, *Phys. Rev. B* **2010**, *81*, 184106-1-15.
- [19] K. Senevirathne, C. S. Day, M. D. Gross, A. Lachgar, N. A. W. Holzwarth, *Solid State Ionics* **2013**, *233*, 95–101.
- [20] A. Gudat, S. Haag, R. Kniep, A. Rabenau, *Z. Naturforsch. B* **1990**, *45*, 111–120.
- [21] J. Cabana, C. D. Ling, J. Oró-Solé, D. Gautier, G. Tobias, S. Adams, E. Canadelli, M. R. Palacin, *Inorg. Chem.* **2004**, *43*, 7050–7060.
- [22] G. Brachtel, R. Hoppe, *Z. Anorg. Allg. Chem.* **1978**, *438*, 97–104.
- [23] R. D. Shannon, *Acta Crystallogr., Sect. A: Cryst. Phys. Diffr. Theor. Gen. Crystallogr.* **1976**, *32*, 751–767.
- [24] G. J. Bullen, F. S. Stephens, R. J. Wade, *J. Chem. Soc. A* **1969**, 1804–1812.
- [25] R. Lauterbach, *Diploma Thesis*, University of Bayreuth, Germany, **1996**.
- [26] B. A. Boukamp, R. A. Huggins, *Mater. Res. Bull.* **1978**, *13*, 23–32.
- [27] W. Schnick, J. Lücke, *Solid State Ionics* **1990**, *38*, 271–273.
- [28] R. Klement, O. Koch, *Chem. Ber.* **1954**, *87*, 333–340.
- [29] A. A. Coelho, *TOPAS Academic*, version 4.1, Coelho Software, Brisbane, Australia, **2007**.
- [30] A. A. Coelho, *J. Appl. Crystallogr.* **2003**, *36*, 86–95.
- [31] a) G. Oszlányi, A. Sütő, *Acta Crystallogr., Sect. A: Found. Crystallogr.* **2004**, *60*, 134–141; b) G. Oszlányi, A. Sütő, *Acta Crystallogr., Sect. A: Found. Crystallogr.* **2008**, *64*, 123–134; c) A. A. Coelho, *Acta Crystallogr., Sect. A: Found. Crystallogr.* **2007**, *63*, 400–406.
- [32] a) R. W. Cheary, A. Coelho, *J. Appl. Crystallogr.* **1992**, *25*, 109–121; b) R. W. Cheary, A. A. Coelho, J. P. Cline, *J. Res. Natl. Inst. Stand. Technol.* **2004**, *109*, 1–25.
- [33] M. Järvinen, *J. Appl. Crystallogr.* **1993**, *26*, 525–531.

Received: November 26, 2014
Published Online: January 9, 2015